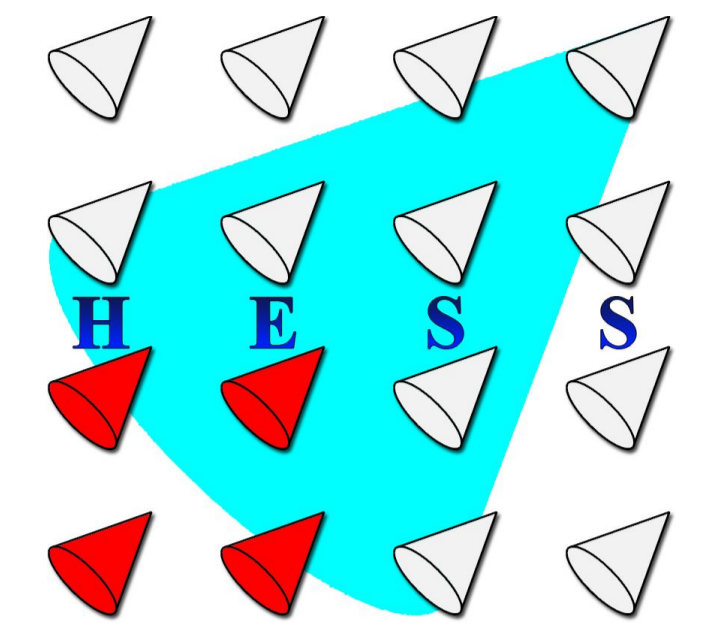


# Upper Limits on the Pulsed VHE $\gamma$ -ray Emission from Two Young Pulsars Investigated with the High Energy Stereoscopic System

A. Noutsos<sup>1,2</sup> for the H.E.S.S. collaboration

<sup>1</sup> Department of Physics, Durham University, South Road, Durham DH1 3LE, UK  
<sup>2</sup> Jodrell Bank, Lower Withington, Macclesfield, Cheshire SK11 9DL, UK



## Abstract

The High Energy Stereoscopic System (H.E.S.S.) is a system of four, imaging, atmospheric Cherenkov telescopes in Namibia, designed to detect very-high-energy  $\gamma$  rays above  $\sim 100$  GeV. During 2002–2003, H.E.S.S. collected data from two, young and energetic radio pulsars: the Crab and PSR B1706–44. We searched for pulsations at the lowest energies that H.E.S.S. is capable of detecting, aiming at a detection that would potentially differentiate between the two popular models of pulsar high-energy emission: the Polar Cap and the Outer Gap. No evidence for pulsed emission was found in the data, and upper limits were derived to a 99.95% confidence level. Our assumptions and upper limit values for the two pulsars are reported.

## The Pulsars

**Crab**  
— Often characterised as the “standard candle”: virtually all efforts to detect its pulsed emission from radio to high-energy (HE  $\geq 100$  MeV)  $\gamma$  rays have been successful.  
— Detected up to  $\sim 20$  GeV with EGRET<sup>1</sup>; but its pulses become undetectable above this energy.  
— No verifiable detection in very high energies (VHE  $\geq 100$  GeV) so far.

**PSR B1706–44**  
— A young, southern-hemisphere pulsar that lies close to the Galactic centre.  
— First discovered in radio, but it also appears as a strong emitter in HE  $\gamma$  rays.  
— EGRET’s detection has provided the only confident high-energy profile so far, although a strong indication of pulsed emission, to a  $4\sigma$  level, was also found with *Chandra*.  
— Above  $\sim 20$  GeV, only upper limits exist for this pulsar.

Table 1. The properties of the Crab and PSR B1706–44 pulsars

	$P$ (s)	$\dot{P}$ ( $10^{-15}$ s s <sup>-1</sup> )	$\log \tau$ (y)	$\log B_p$ (G)	$\dot{E}$ ( $10^{36}$ erg s <sup>-1</sup> )	$\epsilon_\gamma$ % ( $>100$ MeV)
Crab	0.033	421	3.1	12.6	450	$\sim 0.01$
PSR B1706–44	0.102	93	4.2	12.5	3.4	$\sim 0.1$

## The Models

**Polar Cap (PC)**  
— Emission is generated close to the pulsar’s surface, above the polar caps; the main mechanisms are synchrotron and curvature radiation.<sup>3,4</sup>  
— Predicts steep spectral cut-offs at a few GeV.

**Outer Gap (OG)**  
— Emission is generated in the outer magnetosphere, inside charge-depleted regions (gaps); the main mechanisms are synchrotron and curvature radiation, as well as inverse-Compton (IC) upscattering.<sup>5,6</sup>  
— Predicts gentler cut-offs in the GeV range and an additional IC component at TeV energies.

## The Observatory



Name: H.E.S.S. (High Energy Stereoscopic System)<sup>7</sup>  
Location: Khomas highland, Namibia ( $16^\circ 30' 00''$  W,  $23^\circ 16' 18''$  S)  
System: Four imaging Cherenkov telescopes  
Sensitivity (point sources,  $5\sigma$ , 50 h): 0.01 Crab at  $\sim$  TeV – 0.1 Crab at  $\sim$  100 GeV  
Energy range:  $\sim 100$  GeV – 50 TeV

## Observations

**Crab pulsar (observed in 2003)**  
Observing Mode: Stereo (3 telescopes)  
Exposure Time ( $T$ ): 4.5 h of good-quality data were selected based on weather conditions and trigger rate ( $R$ ).  
Zenith Angle (Z.A.):  $45^\circ$ – $60^\circ$

**PSR B1706–44 (observed in 2002)**  
Observing Mode: Single-telescope  
Exposure Time: 28 h  
Zenith Angle:  $< 30^\circ$

Table 2. Analysis parameters and resulting fluxes for the Crab and PSR B1706–44

	$T$ (h)	Z.A.	$R$ (post-cut background) (Hz)	$p_{H-test}$	$\delta$ (% $P$ )	$\nu$	$E_{th}$ (GeV)	$A_{eff}(E_{th})$ (m <sup>2</sup> )	$F_{ul}(>E_{th})$ (cm <sup>-2</sup> s <sup>-1</sup> )
Crab	4.5	$45^\circ$ – $60^\circ$	98	0.29	10	2.08	$232 \pm 51$	$10^4$	$1.8 \times 10^{-10}$
PSR B1706–44	28	$< 30^\circ$	45	0.008	30	2.1	$75 \pm 12$	400	$2.5 \times 10^{-9}$

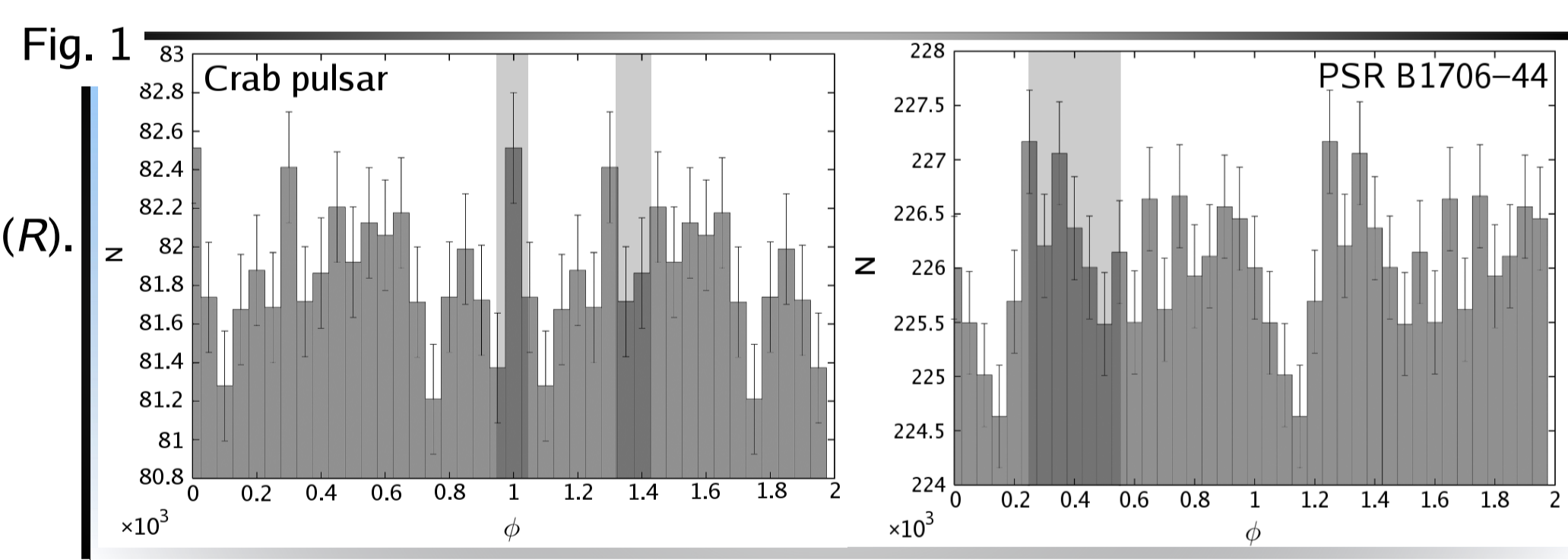
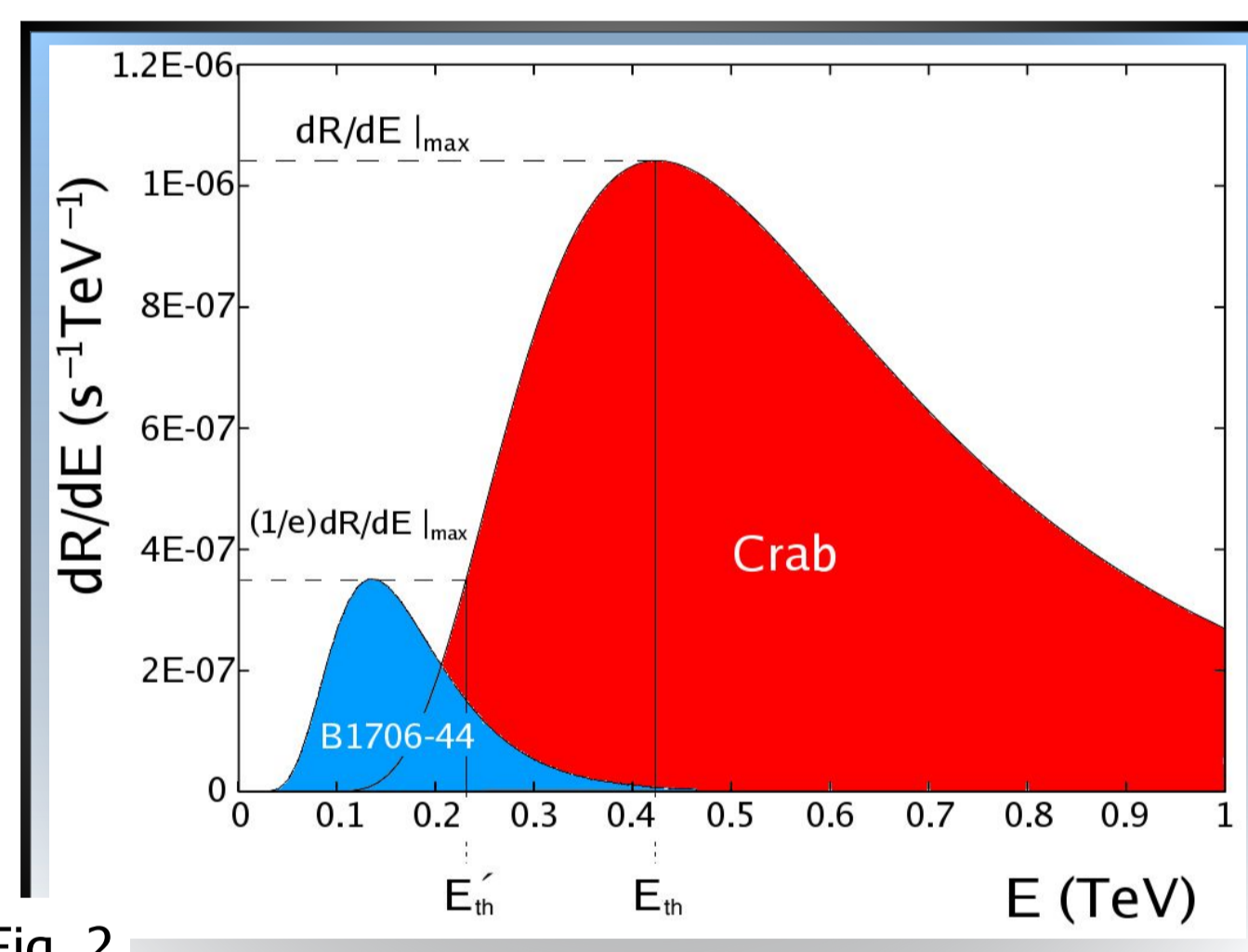
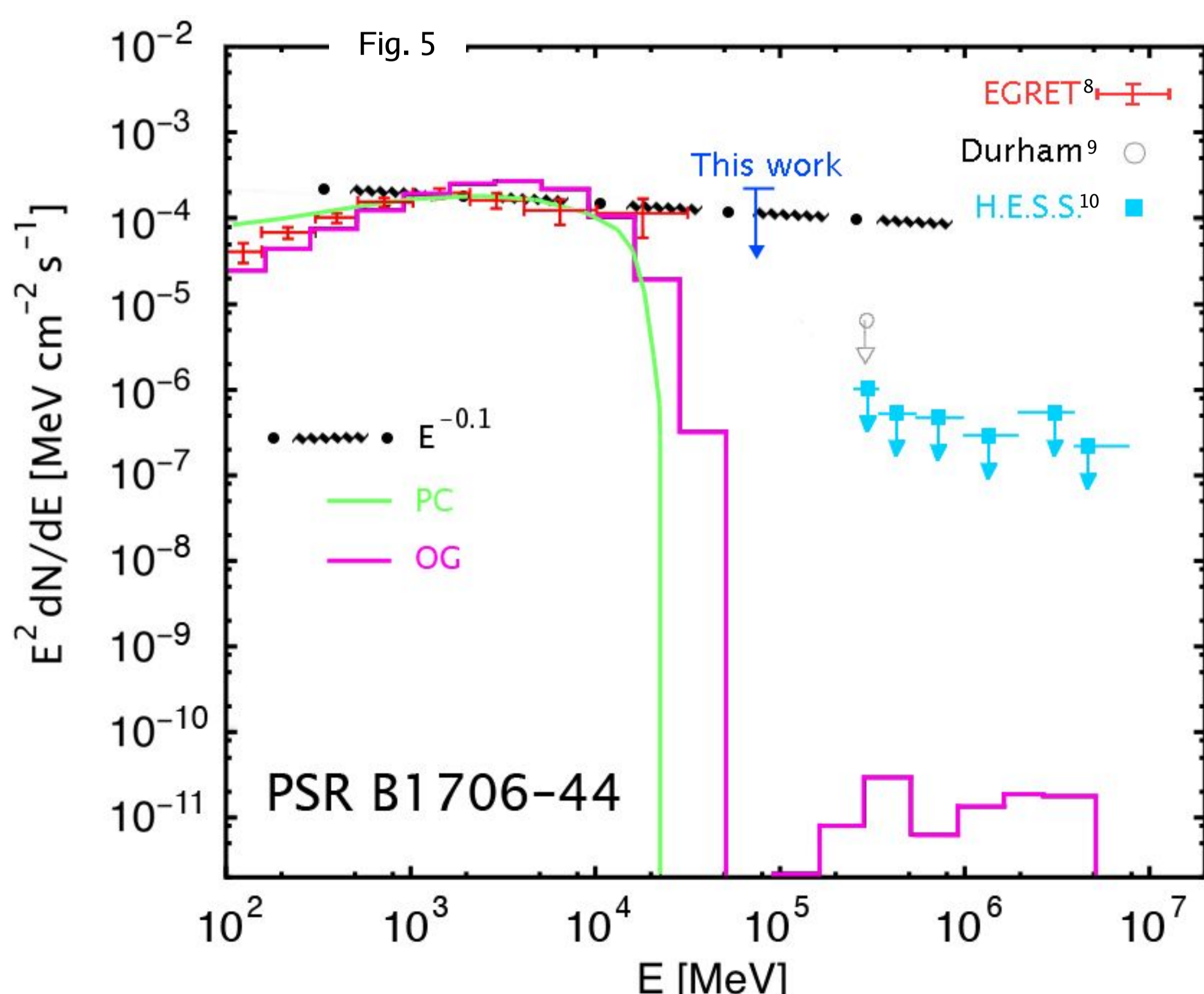
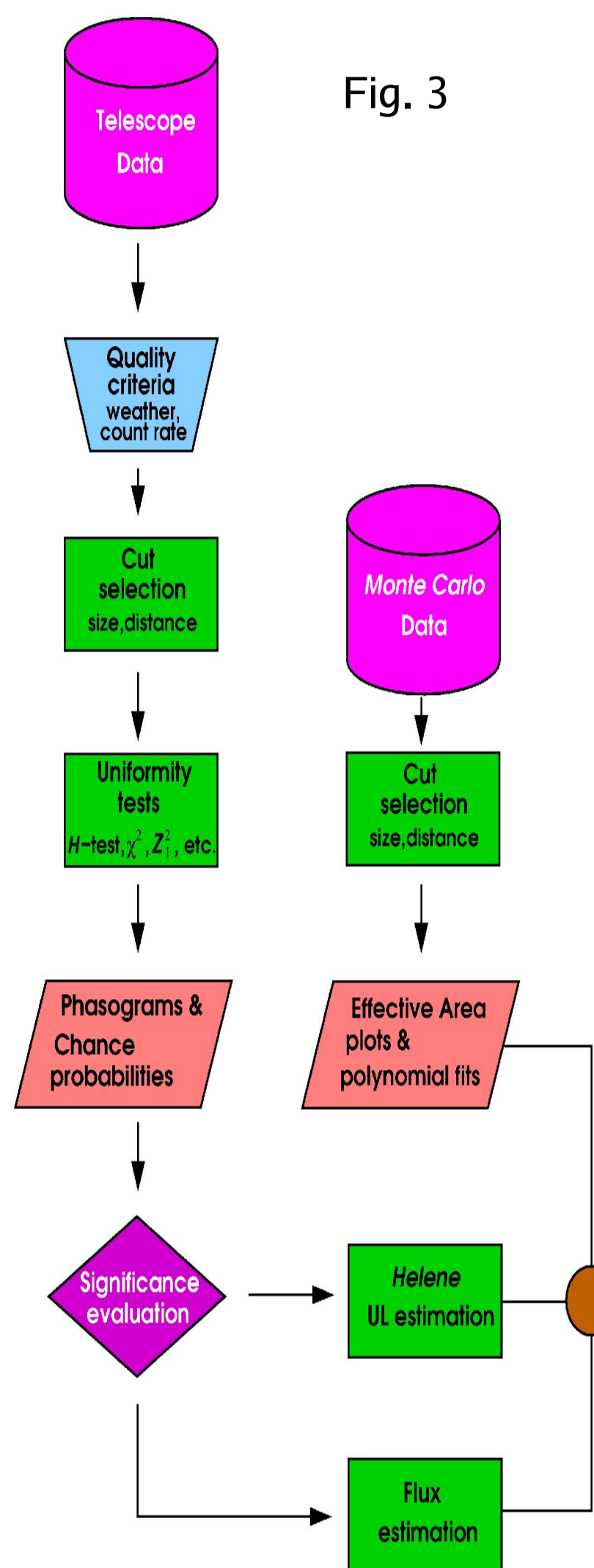


Fig. 3



## Low-energy Analysis

### Objectives

- Sample the lowest energies that H.E.S.S. could detect in the above pulsar observations.
- Intercept the tail-end of the pulsed GeV emission observed with EGRET.
- Constrain the predictions of the PC and OG models using either the  $\gamma$ -ray fluxes, in case of detection, or the upper limits (ULs) on the flux, following a non-detection.

### Strategy

1. We applied specially tailored event-selection cuts to the  $\gamma$ -ray images in order to restrict the data below the standard energy range of the H.E.S.S. analysis: we only accepted events whose total photo-electron (ph.e.) content (size) was below 100 and only those which lay closer than 18-mrad distance on the camera plane, from the source position.
2. The remaining timestamps after the cuts were tested for periodicities using a valid ephemeris and tests like the  $H$ -test<sup>11</sup>,  $\chi^2$ -test, etc.
3. Based on the outcome probabilities ( $p$ ) and phasograms, a choice between signal estimation and UL calculation had to be made: the phasograms (Fig. 1) were consistent with Poissonian background fluctuations, i.e. the lack of significant excess across one period.
4. For the UL calculation, we used the *Helene*<sup>12</sup> method along with a set of assumptions about the spectral shape ( $dN/dE \propto E^{-\nu}$ ) and the duty cycle ( $\delta$ ) of the pulsar’s emission (Table 2).
5. Finally, we calculated  $3\sigma$  differential-flux ULs by convolving the effective area functions ( $A_{eff}$ ) with the assumed spectra above a chosen energy threshold: contrary to the typical definition of the latter, i.e. the energy at the maximum differential rate ( $r_{max} = dR(E_{th})/dE|_{max}$ ), we chose to represent the low-energy data with a threshold,  $E'_{th}$ , where  $dR(E'_{th} < E_{th})/dE = (1/e) r_{max}$ . The differential-rate plots of Fig. 2 justify our decision: a large fraction of the events lie below  $E_{th}$ .

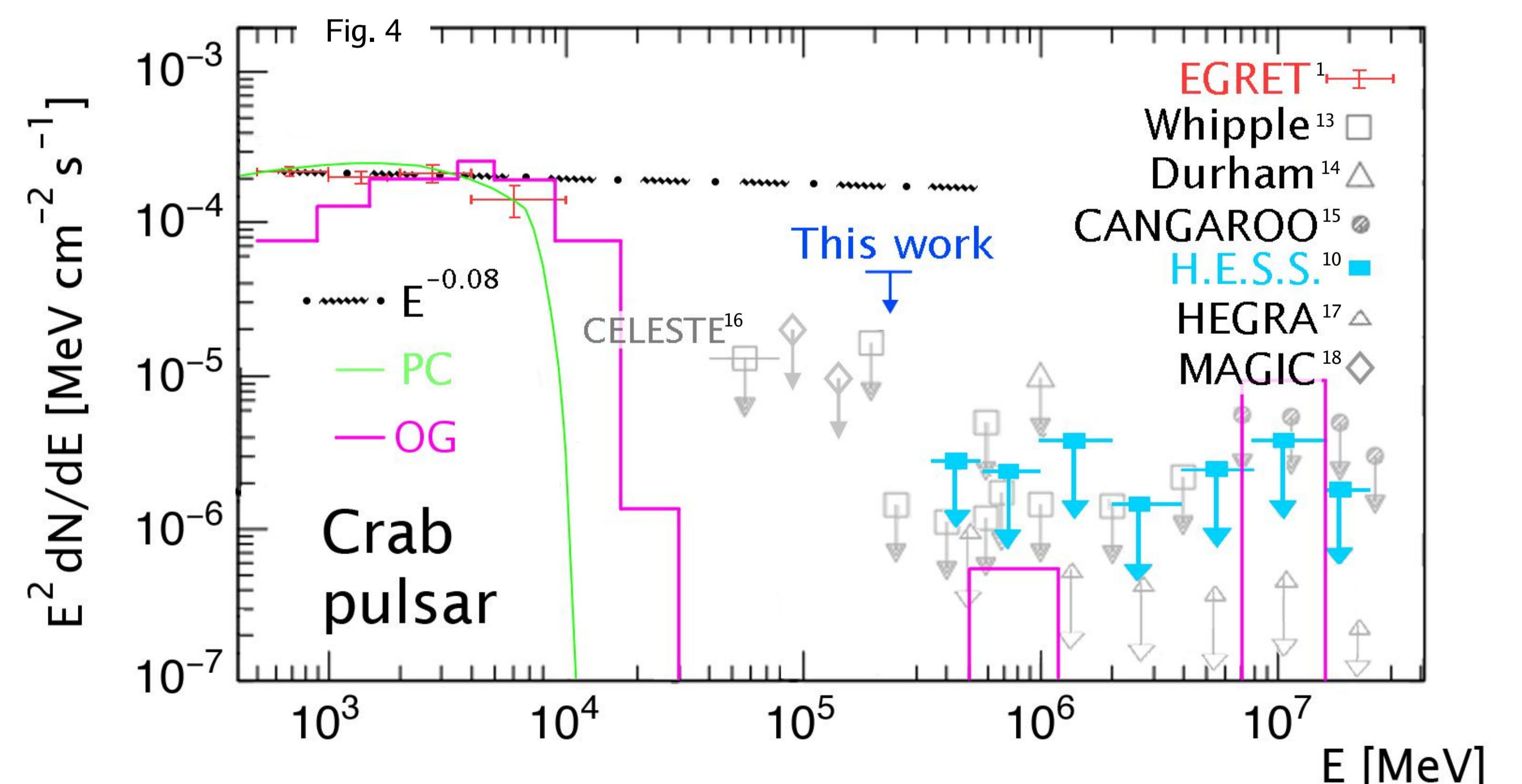
A flowchart of our entire analysis procedure is shown in Fig. 3.

## Results and Conclusions

Figures 4 and 5 show plots of the differential  $\gamma$ -ray flux multiplied by  $E^2$  versus  $E$  for the Crab and PSR B1706–44, respectively:

- Up to  $\sim 20$  GeV there exist confident detections with EGRET (red crosses), whereas at higher energies the emission has only been constrained with upper limits from the various VHE ground-based experiments.
  - ULs based on the standard H.E.S.S. analysis are shown with cyan squares.
  - Shown in blue are our low-energy upper limits; it can be seen that these are well-shifted towards lower energies with respect to those of other experiments. Unfortunately, due to the large background inherent in our analysis, our upper limits are 2–3 orders of magnitude larger than those after the standard H.E.S.S. analysis.
  - The spectral predictions of the PC and OG models for each pulsar are shown with the light green and magenta lines, respectively.
- In the case of the Crab pulsar, the derived ULs can confidently exclude the possibility of a single power law from EGRET’s range to at least  $\sim 230$  GeV, thus verifying the indications for a cut-off already observed at the top energy-bin of EGRET. However, for PSR B1706–44, the large ULs prevent a similar conclusion. One of the main differences between PC and OG spectra is the much steeper cut-offs of the former compared to the latter. The differentiation between the GeV cut-offs of the PC and OG could provide the answer to which model describes pulsar emission best. However, it is clear from Figures 4 and 5 that our ULs, although nearer to the spectral cut-offs than previous H.E.S.S. results, still lack the sensitivity in terms of flux at the required low energies. Hence the problem stands.

Future experiments, like H.E.S.S. Phase II, MAGIC and GLAST, will almost certainly fill the energy gap between HE and VHE observations and, consequently, piece the puzzle of pulsar  $\gamma$ -ray emission.



## References

1. Nolan, P. L. et al., *ApJ*, **409**, 697 (1993)
2. Gotthelf, E. V. et al., *ApJ*, **567**, L125 (2002)
3. Sturrock, P. A., *ApJ*, **164**, 529 (1971)
4. Ruderman, M. A. and Sutherland, P. G., *ApJ*, **196**, 51 (1975)
5. Cheng, K. S., Ho, C. and Ruderman, M. A., *ApJ*, **300**, 500 (1986)
6. Chiang, J. and Romani, R. W., *ApJ*, **400**, 629 (1992)
7. Aharonian, F. et al., *Astropart. Phys.*, **6**, 343 (1997b)
8. Thompson, D. J. et al., *ApJ*, **465**, 385 (1996)
9. Chadwick, P. M. et al., *Astropart. Phys.*, **9**, 131 (1998)
10. Schmidt, F., Master’s Thesis, Humboldt—Universität zu Berlin, Berlin, Germany (2005)
11. de Jager, O. C. et al., *A&A*, **221**, 180 (1989)
12. Helene, O., *Nucl. Instr. & Meth. Phys. Res.*, **212**, 319 (1983)
13. Lessard, R. W. et al., *ApJ*, **531**, 942 (2000)
14. Dowthwaite, J. C. et al., *ApJ*, **286**, L35 (1984)
15. Tanimori, T. et al., *ApJ*, **492**, L33 (1998)
16. de Naurois, M. et al., *ApJ*, **566**, 343 (2002)
17. Aharonian, F. et al., *ApJ*, **614**, 897 (2004)
18. López, M., *29th ICRC, Pune, India*, **4**, 243 (2005)